Photoinduced Orientation of Azobenzene Chromophores in Amorphous Polymers As Studied by Real-Time Visible and FTIR Spectroscopies

T. Buffeteau,*,† F. Lagugné Labarthet,† M. Pézolet,‡ and C. Sourisseau†

Laboratoire de Physicochimie Moléculaire (UMR 5803-CNRS), Université Bordeaux I, 351 cours de la Libération, 33405 Talence, France, and Centre de Recherche en Sciences et Ingénierie des Macromolécules, Département de Chimie, Université Laval, Québec, G1K 7P4, Canada

Received May 28, 1998; Revised Manuscript Received August 6, 1998

ABSTRACT: *In situ* dynamical study of the photoinduced orientation of the DR1 azobenzene derivative in a doped PMMA matrix and in p(DR1A-*co*-MMA) copolymers was carried out using real-time visible and infrared spectroscopies. The different mechanisms occurring during the photoisomerization cycles were highlighted by following the time dependence of the normalized average absorbance (T_0), the normalized linear dichroism (T_2) and the order parameter (P_2) during the orientation (laser on) and the relaxation (laser off) periods. The thermal cis−trans back-relaxation and the angular redistribution were followed separately from the T_0 and T_2 relaxation curves, respectively. The orientation and relaxation curves were fitted by the Kohlrausch−Williams−Watts (KWW) function in order to compare the rate constant and the distribution width for various samples. On one hand, the chromophore−matrix interactions were investigated in doped systems by changing the tacticity of the PMMA matrix. On the other hand, the chromophore−chromophore interactions in functionalized polymers were studied by changing the concentration of azobenzene units in copolymer systems.

Introduction

Azobenzene-containing polymers have a variety of potential applications and have thus received a lot of attention in the past few years.[1] The main interest of these systems is their birefringent properties when they are irradiated with linearly polarized light. This birefringence comes from the reorientation of the azobenzene groups through trans−cis−trans isomerization cycles, which create an excess of photochromic entities oriented perpendicularly to the laser polarization direction. When the laser is turned off, the photoinduced orientation is relatively stable in polymers containing azobenzene side chains (80% of the orientation is preserved),[2,3] while it is less stable in azobenzene-doped polymer matrixes.[4] In this last case, Sekkat et al.[5−7] have proposed the basis of a simple three-level theoretical model in order to explain the reorientation mechanisms of the "azo" molecules during the orientation (laser on) and the relaxation (laser off) processes. In this model, they have considered that the polarized light induces a selective optical pumping ("angular hole-burning") followed by angular reorientations during the trans−cis isomerization and the cis−trans thermal back-relaxation. Moreover, the final orientation distribution of the azobenzene groups with respect to the radiation polarization direction is assumed to be uniaxial. This phenomenological approach explains the reorientation mechanisms of the azo molecules during photoisomerization cycles, and its predictions can be compared with experimental results of the time-dependent orientation and relaxation processes.[3−6]

However, it is not straightforward to understand the time dependence of the photoinduced orientation in azobenzene amorphous polymers because several structural factors may be involved in the reorientation mechanisms. Among these factors, the nature of the neighbors of an azobenzene unit in a functionalized polymer may be quite important. For copolymers containing azobenzene entities and methyl methacrylate structural units, birefringence measurements[2,8] have shown that the degree and rate of ordering are dependent on the distribution of the azobenzene side chains, indicating that azobenzene groups tend to move in concert with each other. More recently, cooperative motions between photoactive and non/photoactive neighbor groups have been observed by analyzing the photoinduced birefringence[9] and also by investigating motions of the molecular groups using real-time infrared spectroscopy.[10,11] These studies clearly indicate that cooperative motions are possible in amorphous polymers, even below T_g, and that the polarity of the groups involved in the cooperative motions is an important factor. Similarly, the photoinduced orientation of azobenzene groups has been used to reorient non photochromic groups in liquid crystalline (LC) polymers[12−15] or to align LC molecules in Langmuir−Blodgett films.[16,17] The nature of the matrix in the doped polymer systems is also a factor that influences the angular reorientation of azobenzene derivatives. Böhm et al.[18] have shown by transient absorption spectroscopy that the kinetics of the relaxation process are very dependent on the matrix rigidity. All studies show that the kinetics of the thermal cis−trans back-relaxation of a chromophore embedded in a polymer matrix differ from the behavior in solution and are very sensitive to the structure, morphology, and viscoelastic properties of the surrounding polymer.[19,20] Nevertheless, the physical meaning of the rate constants of the orientation and relaxation processes must be associated to the photoisomerization mechanisms and to the lifetime of the intermediate metastable cis isomer.

In this paper we have studied the dynamics of the photoinduced orientation of 4′-{[2-hydroxyethyl]ethyl-

* To whom correspondence should be addressed. E-mail: thbuff@lpct.u-bordeaux.fr.
† Université Bordeaux I.
‡ Université Laval.

10.1021/ma980843z CCC: $15.00 © 1998 American Chemical Society
Published on Web 09/26/1998

amino}-4-nitroazobenzene (DR1) in a poly(methyl methacrylate) (PMMA) matrix (DR1−PMMA) and poly{4′-[[2-acryloyloxy-ethyl]ethylamino]-4-nitroazobenzene-*co*-methyl methacrylate} (p[DR1A-*co*-MMA]) using visible and infrared spectroscopies. To analyze the different mechanisms occurring during the photoisomerization cycles, we have calculated the normalized average absorbance (T_0), the normalized linear dichroism (T_2), and the order parameter (P_2). The time dependences of these parameters during the orientation and the relaxation periods are presented for the 492 nm electronic transition and for several vibrational modes. The orientation and relaxation curves of T_0 and T_2 have been fitted by the Kohlrausch−Williams−Watts (KWW) function,[21] the so-called stretched exponential function, to compare the dynamics of various DR1−PMMA and p(DR1A-*co*-MMA) samples. The chromophore-matrix interactions were investigated in the doped systems by changing the tacticity of the PMMA matrix. Finally, the chromophore−chromophore interactions in functionalized polymers were studied by varying the concentration of azobenzene units in various p[DR1A-*co*-MMA] copolymers.

Experimental Section

Materials. The doped polymer samples were obtained by dissolving commercially available Disperse Red 1 (Aldrich, 95% dye content) in chloroform solutions of monodisperse PMMA ($M_w = 120\,000$). Solutions were filtered and deposited by spin coating onto calcium fluoride optical flat windows. Films were then heated for 1 h at 90 °C to remove any remaining solvent. The film thicknesses ranged from 0.8 to 1.2 μm and the dye content was about 5% (w/w). The structural properties of the polymer matrix were modified by changing the stereoregularity of PMMA: various samples were obtained by dispersing DR1 in isotactic and in syndiotactic PMMA.

The synthesis and characterization of p[DR1A-*co*-MMA] copolymers have been described in previous publications.[22−24] Random copolymers with DR1A mole fraction (x) of 0.08, 0.23, 0.44, 0.81, and 1.0 were investigated. To prepare thin films, the copolymers were dissolved in chloroform and the solutions were deposited by spin coating onto barium fluoride optical flat windows. Film thicknesses were between 100 nm ($x = 1$) and 1 μm ($x = 0.08$) in order to have approximately a constant number of chromophores irradiated by the laser beam. The structures of the doped and functionalized polymers are shown in Scheme 1.

Experimental Setup. UV/visible absorption measurements were recorded with a Philips PU8700 spectrometer, using the optical setup previously described.[4] Kinetic measurements were performed in situ by irradiating the sample with a vertically polarized Ar^+ laser light (ILT 5490, $\lambda = 514.5$ nm) and by analyzing the transmitted light using a probe beam (circularly polarized) fixed at the absorption maximum of the sample in the visible region. The transmitted light was then analyzed using a Polaroid film in order to measure the absorbance of the sample in the parallel ($A_\parallel$) and perpendicular ($A_\perp$) directions with respect to the pump laser polarization.

Infrared linear dichroism (IRLD) spectra obtained by polarization modulation (PM) were recorded with either a Nicolet 740 or a Bomem Michelson MB-100 FTIR spectrophotometer using the optical setup and the two channel electronic processing previously described.[3,25] The optical anisotropy in the polymer films was induced in situ using either a polarized Ar^+ laser ($\lambda = 514.5$ nm) in the Nicolet optical setup or a polarized frequency-doubled Nd:YAG laser ($\lambda = 532$ nm) in the Bomem optical setup. In the two cases, the angle between the laser and the infrared beam was 20°. By using a proper calibration procedure,[25] any PM-IRLD spectrum can be related quantitatively to the dichroic difference spectrum $\Delta A = A_\parallel - A_\perp$. The time dependence of the average absorbance was determined from separated conventional measurements of $A_\parallel$ and $A_\perp$. In this case, spectra were corrected for the polymer matrix contribution by subtracting the spectrum of PMMA.

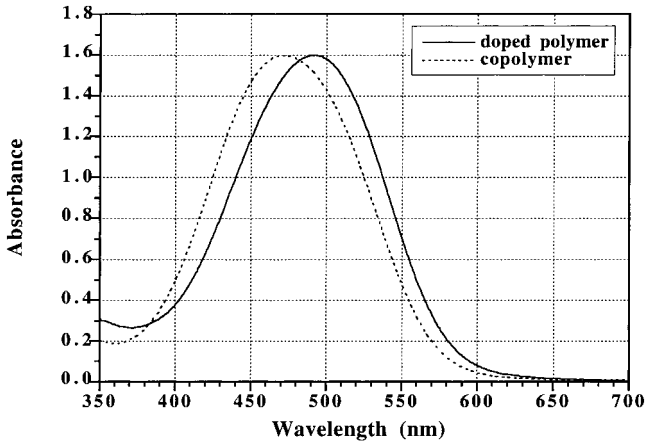

Figure 1. Absorbance spectra in the visible region between 350 and 700 nm of a 5% DR1 doped PMMA film (solid line) and of a p(DR1A-*co*-MMA) copolymer film with a 8% DR1A mole fraction (dashed line).

Scheme 1

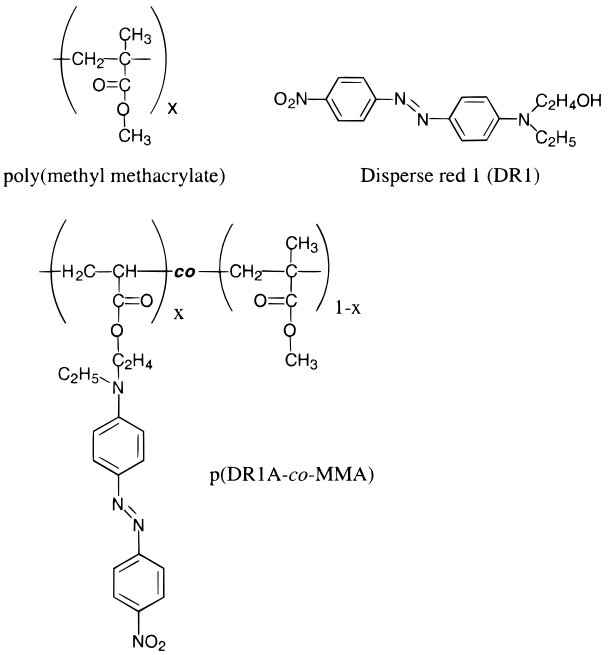

For visible and infrared measurements, the same area was irradiated by the laser beam and the irradiance at the sample was 10 mW/cm^2. Visible measurements and PM-IRLD spectra were collected during the orientation (laser on) and relaxation (laser off) processes. The total acquisition time for the orientation and relaxation kinetics was about 1 h with time resolutions of 5 and 30 s for visible and infrared measurements, respectively.

Results and Discussion

Real-Time UV−Visible Spectroscopy. Figure 1 shows the absorption spectra in the 350−700 nm region of a 5% DR1 doped PMMA film and of a p(DR1A-*co*-MMA) copolymer film with a DR1A mole fraction of 8%. The spectrum of the doped polymer displays a symmetrical intense band at 492 nm due to the vibronically coupled n−π^* and π−π^* electronic transitions.[26,27] The absorption maximum shifts very slightly for low con-

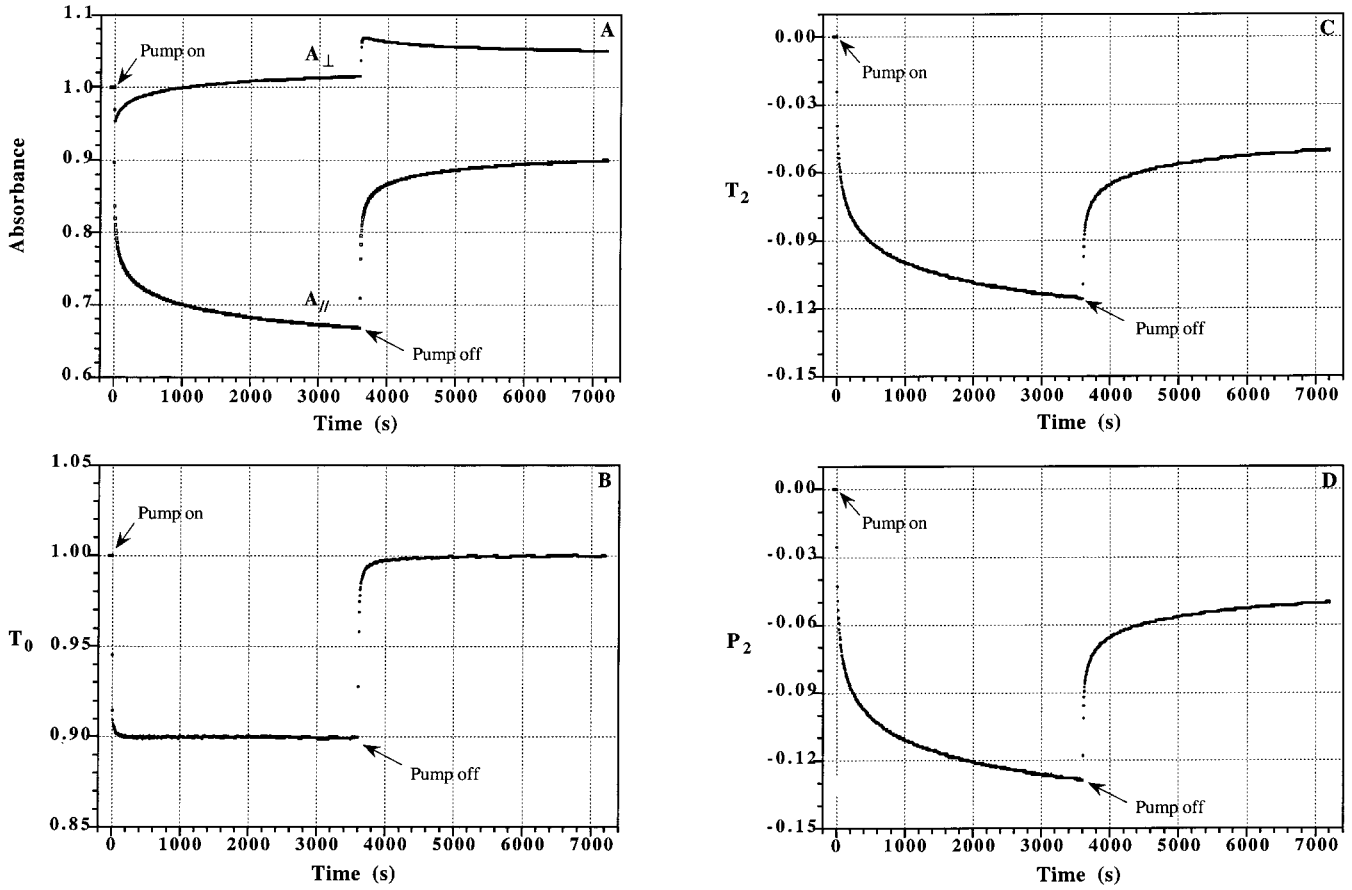

Figure 2. Time dependence of (A) the normalized perpendicular and parallel absorbances, (B) the normalized average absorbance (T_0), (C) the normalized linear dichroism (T_2), and (D) the order parameter (P_2) for the electronic transition at 492 nm of a 5% DR1 doped PMMA film during the orientation (laser on) and relaxation (laser off) periods (I_{pump} = 10mW/cm^2).

centrations of DR1 in PMMA (1 to 10%), as published by Berkovic et al.[28] The spectrum of the copolymer shows also a symmetrical intense band but the absorption maximum is located at a shorter wavelength (λ = 472 nm). Brown et al.[2] have shown that the absorption maximum for copolymers shifts to shorter wavelength as the DR1A mole fraction increases (λ = 455 nm for x = 1.0) and that the electronic absorption band is broader for high azo concentrations. These effects have been attributed to the formation of aggregates in which the dipoles are associated in an antiparallel arrangement.

Typical perpendicular and parallel absorbance variations of a 5% DR1 doped PMMA film during the writing and the relaxation periods are presented in Figure 2A. To compare the time dependence of the two polarization spectra, we have used the normalized absorbances obtained by dividing $A_{||}$ and $A_\perp$ by the absorbance of the film before irradiation, A_0. It appears that at least two regimes are involved in the writing process. The fast one is due to the pump efficiency and depends on both the intensity of the pump laser and the angle between the laser polarization direction and the long molecular axis of the azobenzene groups by a "$I_0 \cos^2 \theta$" factor. This selective optical pumping from the trans-to-cis isomers produces an "angular hole burning" (AHB) in the angular distribution of the trans isomers. This fast hole burning process is clearly evidenced in Figure 2A by the significant decrease, for very short times, of both the $A_{||}$ and $A_\perp$ components. The decrease of the $A_\perp$ component during the first seconds shows that the absorbance of the cis isomer at 492 nm is smaller than that of the trans isomer, as published by Loucif-Saïbi et al.[29] In addition, upon irradiation and during the multiple trans−cis−trans isomerization cycles, there is a slow "angular redistribution" (AR) of the DR1 molecules according to their ability to rotate by thermal random interactions with the host medium and to diffuse by thermal back-relaxation. Consequently, during the writing period, the AHB and AR processes occur simultaneously producing a slight increase in the concentration of DR1 molecules oriented perpendicularly to the laser polarization direction, as shown by the time variations of the $A_{||}$ and $A_\perp$ components.

When the laser is turned off, the thermal cis−trans back-relaxation, which depends on the cis lifetime, is the main factor in the first few seconds and is at the origin of the increase of both $A_{||}$ and $A_\perp$ components. After that, during the relaxation period, the AR process principally governs the perpendicular and parallel absorbance time evolution but the initial isotropic disorder of the azobenzene molecules is never recovered ($A_{||} \neq A_\perp$), even after a long time delay. During this period, the increase of the perpendicular absorbance with respect to the initial absorbance before irradiation, A_0, is approximately equal to half the decrease of the parallel absorbance, revealing a uniaxial orientation of the trans molecules with respect to the laser polarization direction. Under these symmetry considerations, the molecular orientation can be expressed by two parameters: T_0, the normalized average absorbance

$$T_0 = \frac{2A_\perp + A_{||}}{3A_0} \qquad (1)$$

and T_2, the normalized linear dichroism

$$T_2 = \frac{A_{\parallel} - A_{\perp}}{3A_0} \tag{2}$$

The time dependences of the T_0 and T_2 parameters are shown in parts B and C of Figure 2, respectively. When the writing laser is turned on, T_0 decreases during the first few seconds and reaches a plateau value ($\approx$0.9) which is characteristic of a photostationary state. As mentioned above, this very fast process is mainly due to the "angular hole burning" process. The decrease of the normalized average absorbance is essentially related to the cis isomer population which can be estimated using the Fischer approach.[30] In the photostationary state, one can thus estimate a cis isomer population of about 20% in a 5% w/w doped polymer film irradiated with a pump intensity of 10 mW/cm^2. It is noteworthy that this cis population may increase up to 40−50% under high irradiance conditions (100−140 mW/cm^2).[4] When the laser is turned off, T_0 relaxes toward a value of 1.0. This kinetics of T_0 is mainly governed by the thermal cis−trans back-relaxation and consequently by the cis lifetime. We have observed that, for some samples, T_0 does not reach its initial value even after a long relaxation period. This can be explained either by a small proportion of trapped cis isomers in constrained cavities or by a small deviation from the uniaxial model due to the homeotropic orientation of the chromophores perpendicularly to the film plane.

The understanding of the time dependence of the photoinduced linear dichroism T_2 (Figure 2C) is not straightforward. In contrast with the above situation for T_0, the angular redistribution of the DR1 molecules plays an important role in the kinetics of T_2. Indeed, if one considers an isotropic distribution of cis isomers, the time dependence of T_2 is only governed by the orientation changes of the trans molecules. During the writing period, the AR contribution is superimposed to the hole burning process but its effect is emphasized at long times. After 1 h of irradiation, the value of the normalized linear dichroism is approximately −0.11, but the saturation regime is not reached for an irradiance of 10 mW/cm^2 on the sample. Lagugné Labarthet et al.[4] have already shown that an irradiance higher than 100 mW/cm^2 is necessary to obtain the maximum value of linear dichroism. During the relaxation period, the time dependence of T_2 is mainly associated to the angular redistribution of the trans molecules. This relaxation kinetics may be strongly affected by the surrounding matrix (in particular by the different sizes and polarities of the cavities) which limits the total relaxation of the chromophores. Consequently, 50% of the linear dichroism remains after 1 h of relaxation.

Finally, a more general description of the molecular orientation can be obtained by calculating the order parameter, $P_2(\cos\theta)$, which is the second-order coefficient of a series expansion of the orientation distribution.[31,32] The order parameter, associated with the orientation of the transition dipole moment of the electronic transition, is given by the following relation:

$$P_2(\cos\theta) = \frac{T_2}{T_0} = \frac{A_{\parallel} - A_{\perp}}{A_{\parallel} + 2A_{\perp}} \tag{3}$$

The limiting values of $P_2(\cos\theta)$ are +1.0 or −0.5 if the transition moment is perfectly oriented parallel or perpendicular to the polarization direction of the writing laser, respectively; it is equal to zero for random orientation.

Since the cis isomer also absorbs at 492 nm, the order parameter calculated during the orientation period is not representative of only the trans DR1 molecular orientation. In fact, the normalized linear dichroism T_2 is characteristic of the trans molecules (assuming an isotropic distribution of the cis molecules) while the normalized average absorbance T_0 is characteristic of both cis and trans populations. Consequently, the $P_2(\cos\theta)$ values calculated during the orientation period are underestimated and will never reach the limiting value of −0.5 for a transition moment perpendicular to the polarization direction.

Figure 2D shows the time dependence of the order parameter $P_2(\cos\theta)$ associated with the absorption band at 492 nm. At time zero, all the DR1 molecules are randomly distributed in the film and $P_2(\cos\theta)$ is equal to zero. When the linearly polarized laser is turned on, $P_2(\cos\theta)$ becomes negative, showing that the transition dipole moment of the electronic absorption starts moving toward a direction perpendicular to the laser polarization. Since the direction of this transition moment is nearly along the long molecular axis of the DR1 molecules, the polarized laser beam induces a perpendicular orientation of the chromophores, as expected. The P_2 values change drastically for the first few minutes and reach a value of −0.125 after 1 h of irradiation. When the laser is turned off, the system relaxes as shown by the increase of P_2 values but the initial randomness is never achieved under these conditions (the value $P_2(\cos\theta)$ is equal to −0.04 after 1 h of relaxation).

Real-Time Infrared Spectroscopy. The infrared spectra in the 1200−1800 cm^{-1} region of pure PMMA and of the 5% DR1 doped PMMA film recorded before irradiation are presented in Figure 3A. Due to the very low concentration of DR1 in PMMA, the most intense bands come from the PMMA matrix. The very strong band at 1731 cm^{-1} is assigned to the carbonyl stretching vibration ν(C═O). The bands located in the 1350−1500 cm^{-1} region are assigned to the C−H bending vibrations of the α-CH_3 and the O−CH_3 groups whereas the strong bands located in the 1200−1300 cm^{-1} region are due to the asymmetric stretching vibration ν_a(C−C−O) of the ester group.[33−36] The bands associated with the dye molecules are very weak and, in some cases, are masked by the PMMA absorptions. The bands due to the ν_{8a}- and ν_{8b}(C═C) stretching vibrations of the para-substituted phenyl rings are located at 1601 and 1588 cm^{-1}, respectively. The band due to the N═N stretching vibration appears at 1385 cm^{-1} whereas the bands associated with the symmetric $\nu_s(NO_2)$ and antisymmetric $\nu_a(NO_2)$ stretching vibrations of the NO_2 group appear at 1339 and 1519 cm^{-1}, respectively. This last absorption band is overlapped by the ν_{19a}(C═C) stretching vibration of the para-substituted phenyl rings.[37−40]

The PM-IRLD spectrum recorded on the 5% DR1 doped PMMA film irradiated during approximately 1 h is presented in Figure 3B. As seen on the figure, the signal-to-noise ratio of this difference spectrum is remarkable, even though the ΔA for the strongest band is only −0.03. Except for the absorption at 1731 cm^{-1} due to the carbonyl stretching vibration, all the absorption bands of the PMMA matrix have disappeared in the PM-IRLD spectrum, indicating that the orientation

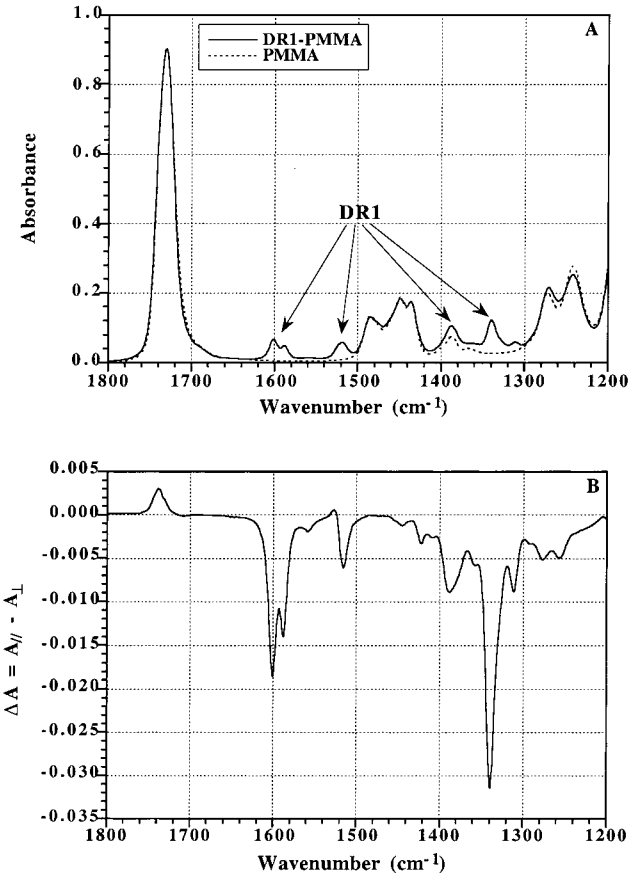

Figure 3. (A) Absorbance spectra in the infrared region between 1200 and 1800 cm^{-1} of a 5% DR1 doped PMMA film recorded before irradiation (solid line) and of pure PMMA (dashed line) and (B) the PM-IRLD spectrum between 1200 and 1800 cm^{-1} of a 5% DR1 doped PMMA film after 1 h of irradiation.

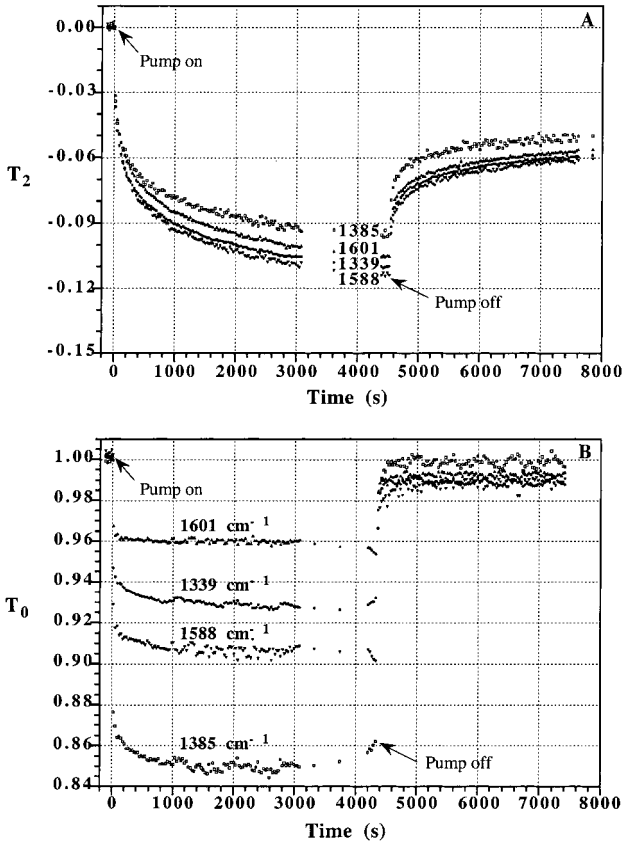

Figure 4. Time dependence of (A) the normalized linear dichroism (T_2) and (B) the normalized average absorbance (T_0) for several infrared bands of a 5% DR1 doped PMMA film during the orientation (laser on) and relaxation (laser off) periods (I_{pump} = 10 mW/cm^2).

of the polymer chains remains isotropic. As a result, all the bands due to the azobenzene molecules are emphasized in the PM-IRLD spectrum. Since the vibrations associated with these bands have their transition dipole moments nearly parallel to the long molecular axis of the dye molecule, their negative signs confirm that irradiation of the film produces a preferential orientation of the DR1 molecules perpendicular to the writing polarization direction, as already shown from visible spectroscopic measurements.

To allow a quantitative comparison of the time dependent behavior of the different bands, the normalized linear dichroism T_2 has been calculated by normalizing the band area in the dichroic difference spectra with the integrated absorbance of the corresponding band in the spectrum recorded before the sample irradiation, A_0 (see eq 2). In Figure 4A, the variation of the T_2 values for several absorption bands of the DR1 molecules is shown as a function of time during the orientation and the relaxation periods. The time dependence of these bands is quite similar to that presented above for the visible region. The maximum values obtained after 1 h of irradiation are close for all the studied bands and are between −0.09 for the ν(N=N) vibration and −0.11 for the $\nu_s(NO_2)$ mode. The similar values obtained for the $\nu_s(NO_2)$ (1339 cm^{-1}) and the stretching vibrations of the para-substituted phenyl rings (1601 and 1588 cm^{-1}) indicate that the direction of their transition dipole moment with respect to the molecular axis of the DR1 molecule is approximately the same. It is interesting to note that the T_2 values of the ν(N=N) and the $\nu_s(NO_2)$ vibrations are close even though their transition dipole moment should make an angle of 60°. This is due to the fact that the ν(N=N) mode is not a pure N=N stretching vibration but is most likely coupled with the ϕ−N stretching vibration because of the electron delocalization along the azobenzene molecule in the trans configuration. This vibrational coupling would move the transition dipole moment of this vibration toward the molecular axis of the DR1 molecule.

Unfortunately, the PM-IRLD spectroscopy does not allow the determination of T_0 since the $A_{\parallel}$ and $A_{\perp}$ absorbances are not recorded separately. The time dependence of the normalized average absorbance has thus been determined by recording $A_{\parallel}$ and $A_{\perp}$ in a conventional manner. Figure 4B shows the variation of T_0 (calculated from eq 1) for several vibrations of the DR1 molecules during the orientation and the relaxation periods. This figure shows that the dispersion of the data on the T_0 curves is more important than that on the T_2 curves. This is due to the fact that the spectra used to calculate T_0 are recorded sequentially (instead of simultaneously for the T_2 curves) and that they have to be corrected for the spectral contribution of the PMMA matrix. As seen in Figure 4B, the normalized average absorbance of all the studied infrared bands decreases during the orientation period and relaxes to almost its initial value when the laser is turned off, as observed for the visible absorption band in Figure 2B. The behavior of T_0 during the polymer irradiation is

Table 1. Parameters Obtained by Fitting the Visible Spectroscopy Relaxation Curves (T_0) with eq 4[a]

sample	A	B	k_r (s^{-1})	β_r	$\langle k_r \rangle$ (s^{-1})
DR1 in atactic PMMA	0.999 ± 0.002	−0.103 ± 0.008	0.107 ± 0.020	0.362 ± 0.018	0.0238
DR1 in syndiotactic PMMA	0.996 ± 0.001	−0.099 ± 0.002	0.072 ± 0.015	0.350 ± 0.005	0.0143
DR1 in isotactic PMMA	1.000 ± 0.001	−0.061 ± 0.005	0.119 ± 0.020	0.350 ± 0.005	0.0237
p(DR1A-*co*-MMA) 8%	1.000 ± 0.001	−0.130 ± 0.002	0.024 ± 0.001	0.396 ± 0.004	0.0070

[a] The fits were realized over a 3050 s time range with a time resolution of 5 s.

most likely due to the fact that the molar absorptivity of the infrared vibrations of the cis isomers is significantly smaller than that of the bands of the trans isomers. On the other hand, the decrease in T_0 is not the same for all vibrations, revealing that the presence of the cis isomers does not have the same effect on their transition dipole moment. In addition, the strong decrease of T_0 at 1385 cm^{-1} may be due to the fact that the ν(N=N) band for the cis isomers is expected to appear at a different wavenumber around 1510 cm^{-1}.[40] The 15% decrease of T_0 would then correspond directly to the percentage of the cis isomers, a value comparable to that obtained by visible absorption spectroscopy. Since T_0 is not equal to 1.0 for the infrared bands in photoinduced orientation studies, the T_2 parameter determined by PM-IRLD does not correspond to the order parameter $P_2(\cos\theta)$ as opposed to results obtained on molecular orientation studies in stretched polymer samples.[25]

Quantitative Analysis of the Orientation and Relaxation Processes. In functionalized polymers, Natansohn et al.[2,41,42] have shown that the time dependence of the birefringence during the orientation and relaxation periods can be quite well described by biexponential functions. The "fast" response modes were associated with dipole reorientations through trans−cis−trans isomerization for the orientation process and with the thermal cis−trans back-relaxation and the angular redistribution of dipoles for the relaxation process. The "slow" response mode for both the orientation and relaxation processes was associated with the dipole reorientations involving motions of the main chain of the polymer. More recently, it has been shown[3] from PM-IRLD measurements that, although the maximum induced orientation of the polymer chain is much smaller than that of the photoactive side chains (azo groups), the kinetics of orientation of the side chains and the polymer chain, and in particular the values of their rate constants, are nearly the same. This shows unambiguously that the "slow" and "fast" modes cannot be separately associated with motions of the main chain and the side chains of the polymer, respectively. In fact, both response modes must be associated with the trans−cis−trans photoisomerization and the biexponential approach is more likely to reflect the dynamics of the azo groups in different environments. Indeed, similar conclusions were reached from real-time spectroscopic measurements on DR1-doped polymer systems,[4] in which the time dependences of T_0 and T_2 during the relaxation period were satisfactorily fitted by biexponential functions; the observation of similar ratios of the "fast" and "slow" rate constants in both cases has suggested that the distribution of chromophores in various surroundings were probed.

Therefore, the KWW function seems to be a more appropriate function to model the dynamics of the chromophores because a distribution of the rate constants is taken into account. The KWW function has been extensively used to model the relaxation of azo molecules in amorphous polymers from dielectric and second harmonic generation measurements,[43−46] to investigate the dynamics of photoinduced isomerization of azobenzene moieties in liquid-crystalline polymers from forced Rayleigh scattering measurements,[47] and to study the dynamics of copolymers containing two types (one polar and another one less polar) of azobenzene side chains from birefringence measurements.[48]

The relaxation curves were thus fitted by the function

$$y(t) = A + B \exp[-(k_r t)^{\beta_r}] \tag{4}$$

where y is either T_0, T_2, or P_2, A is the residual orientation after relaxation, $A + B$ is the induced orientation just before the laser beam is turned off (i.e. in the photostationary state), and k_r and β_r are KWW parameters; k_r represents the rate constant of either the thermal cis−trans back-relaxation process for the T_0 parameter, the angular redistribution process for the T_2 parameter, or both processes for the P_2 parameter; β_r can take values between 0 and 1; $\beta_r = 1$ corresponds to a single-exponential relaxation process while $\beta_r < 1$ indicates a distribution of the relaxation rate constants.

Similarly, the orientation curves of the T_2 parameter have been fitted by the function

$$y(t) = C\{1 - \exp[-(k_w t)^{\beta_w}]\} \tag{5}$$

where C is the maximum achievable orientation, k_w represents the rate constant of dipole reorientations through trans−cis−trans isomerization, and β_w is the width of the distribution of the orientation rate constants.

To compare the orientation and relaxation dynamics in various samples, an average rate constant $\langle k \rangle$ can be defined as[43−46]

$$\frac{1}{\langle k \rangle} = \int_0^\infty \exp[-(kt)^\beta]\, dt = \frac{\Gamma(1/\beta)}{k\beta} \tag{6}$$

where Γ is the gamma function.

Since during the relaxation period the thermal cis−trans back-relaxation and the angular reorientation processes can be separately followed from the time dependence of T_0 and T_2, respectively, the corresponding relaxation curves were first fitted by eq 4. The P_2 relaxation curves, that depend on both processes, were not fitted because the fit parameters have no real physical meaning. For the orientation period, only the T_2 curves were fitted since the time resolution of the experiments was not good enough to obtain a reliable fit of the T_0 curves.

(a) Relaxation Behaviors. The best fit parameters calculated from the T_0 relaxation curves obtained by visible spectroscopy over a 3050 s time range in various samples are summarized in Table 1. As seen in this table, the tacticity of the polymer has only a slight effect on the KWW parameters. The thermal cis−trans back-relaxation rate constant, k_r, is on average equal to 0.1

Table 2. Parameters Obtained by Fitting the Relaxation Curves (T_2) with eq 4[a]

A. Visible Experiments (Time Resolution of 5 s)

sample	*A*	*B*	k_r (s^{-1})	β_r	$\langle k_r \rangle$ (s^{-1})	A_n
DR1 in atactic PMMA	-0.0428 ± 0.0033	-0.0760 ± 0.0022	0.0049 ± 0.0006	0.286 ± 0.009	0.00042	0.36 ± 0.02
DR1 in syndiotactic PMMA	-0.0358 ± 0.0017	-0.0590 ± 0.0020	0.0033 ± 0.0001	0.296 ± 0.013	0.00034	0.38 ± 0.02
DR1 in isotactic PMMA	-0.0712 ± 0.0044	-0.1056 ± 0.0017	0.0011 ± 0.0001	0.368 ± 0.003	0.00026	0.40 ± 0.02
p(DR1A-*co*-MMA) 8%	-0.0909 ± 0.0044	-0.0561 ± 0.0009	0.0013 ± 0.0002	0.305 ± 0.004	0.00015	0.62 ± 0.02

B. Infrared Experiments (Time Resolution of 30 s)

sample	A	B	k_r (s^{-1})	β_r	$\langle k_r \rangle$ (s^{-1})	A_n
Doped Polymer: DR1 in atactic PMMA						
1601 cm^{-1}	-0.0466 ± 0.0049	-0.0587 ± 0.0024	0.0019 ± 0.0003	0.308 ± 0.006	0.00023	0.44 ± 0.03
1588 cm^{-1}	-0.0500 ± 0.0043	-0.0641 ± 0.0028	0.0020 ± 0.0003	0.307 ± 0.005	0.00024	0.44 ± 0.03
1385 cm^{-1}	-0.0396 ± 0.0034	-0.0557 ± 0.0031	0.0019 ± 0.0003	0.280 ± 0.004	0.00015	0.42 ± 0.03
1339 cm^{-1}	-0.0488 ± 0.0045	-0.0610 ± 0.0027	0.0020 ± 0.0002	0.307 ± 0.004	0.00024	0.44 ± 0.03
Functionalized Polymer: p(DR1A-*co*-MMA)						
8%, 1339 cm^{-1}	-0.0826 ± 0.0042	-0.0711 ± 0.0029	0.0006 ± 0.0002	0.308 ± 0.010	0.00007	0.54 ± 0.02
23%, 1339 cm^{-1}	-0.0461 ± 0.0022	-0.0456 ± 0.0015	0.0012 ± 0.0002	0.285 ± 0.010	0.00010	0.50 ± 0.02
44%, 1339 cm^{-1}	-0.0491 ± 0.0025	-0.0330 ± 0.0010	0.0013 ± 0.0003	0.276 ± 0.010	0.00009	0.60 ± 0.02
81%, 1339 cm^{-1}	-0.0665 ± 0.0032	-0.0262 ± 0.0009	0.0013 ± 0.0002	0.281 ± 0.005	0.00010	0.72 ± 0.02
100%, 1339 cm^{-1}	-0.0674 ± 0.0035	-0.0239 ± 0.0006	0.0014 ± 0.0002	0.284 ± 0.005	0.00012	0.74 ± 0.01

[a] The fits were realized over a 3050 s time range.

s^{-1} (i.e. time constant $\tau_{cis} \approx 10$ s) and the β_r parameter of the stretched exponential function is approximately equal to 0.35. The value of the thermal cis−trans back-relaxation rate constant is of the same order of magnitude as that obtained by Barrett et al.[8,49] on various polymers using a pump/relax procedure. However, the reported faster rate constant (i.e. $k_r = 0.36\ s^{-1}$) obtained for 10% DR1 in PMMA could be due to the fact that the fits were realized over a very short temporal range (12 s) as compared to that used in this study.

The KWW parameters for the functionalized copolymer (p(DR1A-*co*-MMA) with 8% mole fraction of DR1A) are quite different. The thermal cis−trans back-relaxation rate constant is approximately four times smaller than that observed in doped polymer systems while the width of its distribution is slightly narrower ($\beta_r = 0.40$). These results indicate that the thermal cis−trans back-relaxation is more hindered in functionalized systems because of the covalent bonding between the azobenzene group and the polymer chain. Finally, it should be noted that in all the investigated samples, the *A* parameter value (normalized average absorbance at infinite time) does not significantly deviate from 1.0, indicating that the uniaxial model used to describe the photoinduced orientation of the chromophores is always valid.

The best fit parameters obtained from the T_2 relaxation curves over a 3050 s time range are summarized in parts A and B of Table 2 for visible and infrared measurements, respectively. The KWW parameters calculated from the results of the visible experiments change with the tacticity of PMMA. The rate constant for the angular redistribution (AR) of trans DR1 molecules is much smaller than that of thermal cis−trans back-relaxation, as predicted in the three-level model by Dumont et al.[5,6] The value of k_r is approximately equal to 0.005 for DR1 in atactic PMMA and is smaller for stereoregular polymers, in particular when all the ester groups are situated on the same side of the chain (isotactic PMMA). This result can be explained by important intermolecular interactions between the chromophores and the polar groups of the surrounding matrix. The β_r parameter is equal to 0.29 for both the atactic and syndiotactic PMMA while it is equal to 0.37 for isotactic PMMA. This large value of β_r in isotactic PMMA reflects a narrowing in the distribution of the AR rate constants due to a specific ordering of the ester groups. The fraction of residual orientation after relaxation, $A_n = A/(A + B)$, appears relatively constant at approximately 0.38 in the doped polymer systems. On the other hand, the A_n value is quite large ($A_n = 0.62$) for the functionalized system. This value is in agreement with those obtained by Brown et al.[2] from birefringence measurements on p(DR1A-*co*-MMA) copolymers with a very low concentration of azo groups. This large value of A_n can be explained by the fact that only some of the azo groups (at the end of the chains, for example) may have more free volume available, as opposed to the situation in doped polymer systems where DR1 molecules relax in surrounding cavities. Moreover, the motions of the side chains may be affected by the main chains of the polymer, as indicated by the smaller value of the AR rate constant in the functionalized system.

The parameters obtained by fitting the infrared T_2 relaxation curves are presented in Table 2B for several vibrations in the 5% DR1 atactic PMMA sample. Within the experimental errors, the rate constants, the widths of distribution, and the fractions of the remaining induced orientation after relaxation are the same for all studied vibrations. The dynamics of the transition dipole moments associated to different parts of the DR1 molecules appear similar even though the magnitudes and the directions of the transition dipole moment may be different. This result indicates that a rodlike symmetry must be considered during the angular redistribution of the DR1 molecules. A puzzling feature of the results presented in Table 2 is the fact that, for the same sample, the k_r values obtained by infrared spectroscopy are nearly two times smaller than those obtained by visible spectroscopy. Such a discrepancy could be explained by the difference in the nature of the transition dipole moments in visible and infrared spectroscopies. Indeed, the electronic transition in the visible region is governed by a very large variation of the dipole moment in a relatively long time scale (≈10−500 ps) in such hyperpolarizable azo derivatives while the intensities of the vibrational modes are associated

Table 3. Parameters Obtained by Fitting the Orientation Curves (T_2) with eq 5[a]

A − Visible Experiments (Time Resolution of 5 s)

sample	C	k_w (s^{-1})	β_w	$\langle k_w \rangle$ (s^{-1})
DR1 in atactic PMMA	-0.1346 ± 0.0036	0.0030 ± 0.0005	0.277 ± 0.006	0.00022
DR1 in syndiotactic PMMA	-0.1215 ± 0.0027	0.0009 ± 0.0001	0.265 ± 0.006	0.00005
DR1 in isotactic PMMA	-0.1685 ± 0.0054	0.0048 ± 0.0003	0.679 ± 0.024	0.00368
p(DR1A-*co*-MMA) 8%	-0.1453 ± 0.0044	0.0070 ± 0.0009	0.517 ± 0.014	0.00372

B − Infrared Experiments (Time Resolution of 30 s)

sample	C	k_w (s^{-1})	β_w	$\langle k_w \rangle$ (s^{-1})
Doped Polymer: DR1 (5%) in atactic PMMA				
1601 cm^{-1}	-0.1236 ± 0.0064	0.0015 ± 0.0003	0.336 ± 0.012	0.00026
1588 cm^{-1}	-0.1315 ± 0.0065	0.0018 ± 0.0003	0.329 ± 0.013	0.00028
1385 cm^{-1}	-0.1170 ± 0.0031	0.0015 ± 0.0003	0.288 ± 0.013	0.00013
1339 cm^{-1}	-0.1289 ± 0.0036	0.0018 ± 0.0003	0.318 ± 0.011	0.00025
Functionalized Polymer: p(DR1A-*co*-MMA)				
8%, 1339 cm^{-1}	-0.1520 ± 0.0024	0.0111 ± 0.0010	0.585 ± 0.030	0.0071
23%, 1339 cm^{-1}	-0.0962 ± 0.0050	0.0343 ± 0.0030	0.652 ± 0.030	0.0252
44%, 1339 cm^{-1}	-0.0857 ± 0.0037	0.0329 ± 0.0030	0.632 ± 0.030	0.0233
81%, 1339 cm^{-1}	-0.0932 ± 0.0015	0.0266 ± 0.0025	0.590 ± 0.020	0.0173
100%, 1339 cm^{-1}	-0.0917 ± 0.0035	0.0241 ± 0.0024	0.520 ± 0.020	0.0129

[a] The fits were realized over a 3600 s time range.

with weak variations with respect to the normal coordinates over a typical picosecond time scale. In the former case, strong long range dipolar interactions between inhomogeneously distributed chromophores can thus be effective and collective effects could be more efficient in the angular reorientation processes and lead to an increase in the apparent rate constant values.

We have also reported in Table 2B the relaxation parameters of the $\nu_s(NO_2)$ vibration for different compositions of p(DR1A-*co*-MMA) copolymers. Since the dynamical parameters are very sensitive to the film thickness, only samples with a similar optical density can be compared;[50] consequently, lower concentrations of the azo species require thicker films. To minimize this effect, the parameters reported for each composition are the average of those calculated from at least five samples of similar thicknesses and the optical density of the $\nu_s(NO_2)$ band ranged from 0.12 to 0.16. The KWW parameters appear essentially constant with the dye concentration ($k_r \approx 0.0013$ and $\beta_r \approx 0.28$), excluding the 8% copolymer sample which displays a smaller rate constant value ($k_r = 0.0006$) and a slightly narrower width of distribution ($\beta_r = 0.31$). On the other hand, the fraction of the remaining induced orientation after relaxation seems to be more affected by the sequence distribution of the copolymer. The A_n parameter varies from 0.5 at low azo concentration to 0.74 for the homopolymer.

(b) Orientation Behaviors. The best fit parameters obtained from the T_2 orientation curves over a 3600 s time range are summarized in parts A and B of Table 3 for visible and infrared measurements, respectively. The k_w rate constants obtained from visible experiments vary with the tacticity of the PMMA, while the β_w value is approximately 0.27, except for the sample of DR1 in isotactic PMMA in which the distribution is very narrow ($\beta_w = 0.68$). In this last sample, the maximum achievable orientation (C parameter) is by far more important in absolute value than in the other doped or functionalized polymer samples. Therefore, the isotactic PMMA is the more appropriate matrix to achieve better orientation of the DR1 molecules; this result is certainly due to the higher mobility of the polymer chains in the isotactic polymer.[51] Indeed, it is expected that the lower the molecular weight and the glass transition temperature (T_g) of a polymer the easier are the polymer chain motions. This explanation is reinforced by considering the physical properties of the studied PMMA: the stereoregular PMMA's have comparable molecular weights ($M_w \approx 40\,000$) while the atactic PMMA has a larger one ($M_w = 120\,000$) and the glass transition temperatures are 60, 114, and 130 °C in isotactic, atactic, and syndiotactic PMMA, respectively.

The parameters calculated from infrared measurements are presented in Table 3B for several vibrations of 5% DR1 in atactic PMMA. The writing rate constants and the widths of distribution are similar for all the studied vibrations while the maximum achievable orientations differ slightly. Such a low dispersion in the C parameter indicates that the transition dipole moments of the studied vibrations have nearly the same orientation due to the strong charge delocalization in the DR1 molecules.

The parameters obtained by fitting the orientation curves of p(DR1A-*co*-MMA) copolymers with different azo concentrations show that the writing dynamics are affected by the sequence distributions in the polymers. The values of the writing rate constant and the width of distribution are maximum for midrange azo concentrations ($x = 0.23$ and $x = 0.44$) while they are minimum at low azo concentration. The increase in the value of the writing rate constant at $x = 0.23$ can be explained by strong dipolar interactions between azo groups inducing collective motions of the side chains. The fact that the k_w value is not maximum for the higher azo concentrations is certainly due to the antiparallel arrangement of the chromophores, as mentioned by Brown et al.,[2] which minimizes the dipolar interactions between chromophores. Finally, the maximum achievable induced orientation is constant for midrange and high-range concentrations of azo groups ($C = -0.090 \pm 0.005$) while it is larger in absolute value for the lowest azo concentration ($C = -0.152$). This result is in good agreement with that extracted from the plot of birefringence per dipole group as a function of azo concentration already reported in reference 2. All these studies thus confirm that an isolated azo group orient better than the azo groups involved in diads and triads, i.e., those with neighboring side chains.[2]

Conclusions

The dynamics of photoinduced orientation in DR1-doped PMMA and in p(DR1A-*co*-MMA) copolymers has been studied in situ by real-time visible and infrared spectroscopies. The use of these spectroscopic techniques has allowed to follow the time dependence of the normalized average absorbance (T_0) and linear dichroism (T_2) during both the orientation and relaxation periods. From these results, we have characterized the different mechanisms associated with the azobenzene photoisomerization, namely the angular hole burning, the angular redistribution, and the thermal cis−trans back-relaxation. In particular, the thermal cis−trans back-relaxation and the angular redistribution were followed separately from the T_0 and T_2 relaxation curves, respectively. The orientation and relaxation curves were fitted by stretched exponential functions in order to obtain quantitative information about the rate constants of the different processes and about their width of distribution.

The results obtained by visible spectroscopy show that the thermal cis−trans back-relaxation is at least 20 times faster than that of the angular redistribution of trans DR1 molecules. In addition, the study of the effect of PMMA tacticity on the relaxation and orientation curves demonstrates that isotactic PMMA is the more appropriate matrix to achieve better orientation of the DR1 molecules. The results obtained by infrared spectroscopy reveal that different chemical groups of the azobenzene molecules display a similar dynamics during both the orientation and relaxation periods, indicating that the DR1 molecules move as a whole units. The study of p(DR1A-*co*-MMA) copolymers shows that isolated azo groups orient more readily than those involved in diads or triads, i.e., in strong chromophore−chromophore interactions.

Acknowledgment. The authors are indebted to the CNRS (Chemistry Department) and to the Région Aquitaine for financial support. They are also thankful to A. Natansohn for providing the functionalized polymers, to Y. Grohens for providing the syndiotactic and atactic PMMA and to P. Rochon for several fruitful discussions.

References and Notes

(1) Xie, S.; Natansohn, A.; Rochon, P. *Chem. Mater.* **1993**, *5*, 403.
(2) Brown, D.; Natansohn, A.; Rochon, P. *Macromolecules* **1995**, *28*, 6116.
(3) Buffeteau, T.; Pézolet, M. *Appl. Spectrosc.* **1996**, *50*, 7.
(4) Lagugné Labarthet, F.; Sourisseau, C. *New J. Chem.* **1997**, *21*, 879.
(5) Sekkat, Z.; Dumont, M. *Synth. Met.* **1993**, *54*, 373.
(6) Dumont, M.; Hosotte, S.; Froc, G.; Sekkat, Z. *SPIE Proc.* **1993**, *2042*, 2.
(7) Sekkat, Z.; Wood, J.; Knoll, W. *J. Phys. Chem.* **1995**, *99*, 17226.
(8) Barrett, C.; Natansohn, A.; Rochon, P. *Macromolecules* **1994**, *27*, 4781.
(9) Meng, X.; Natansohn, A.; Barrett, C.; Rochon, P. *Macromolecules* **1996**, *29*, 946.
(10) Buffeteau, T.; Natansohn, A.; Rochon, P.; Pézolet, M. *Macromolecules* **1996**, *29*, 8783.
(11) Natansohn, A.; Rochon, P.; Pézolet, M.; Buffeteau, T.; Meng, X. *SPIE Proc.* **1997**, *2998*, 185.
(12) Anderle, K.; Birenheide, R.; Werner, M. J. A., Wendorff, J. H. *Liquid Crystals* **1991**, *9*, 691.
(13) Wiesner, U.; Reynolds, N.; Boeffel, C.; Spiess, H. W. *Makromol. Chem., Rapid Commun.* **1991**, *12*, 457.
(14) Wiesner, U.; Reynolds, N.; Boeffel, C.; Spiess, H. W. *Liq. Cryst.* **1992**, *11*, 251.
(15) Stumpe, J.; Läsker, L.; Fischer, Th.; Rutloh, M.; Kostromin, S.; Ruhmann, R. *Thin Solid Films* **1996**, *284−285*, 252.
(16) Seki, T.; Sakuragi, M.; Kawaniski, Y.; Suzuki, Y.; Tamaki, T.; Fukuda, R.; Ichimura, K. *Langmuir* **1993**, *9*, 211.
(17) Seki, T.; Ichimura, K.; Fukuda, R.; Tanigaki, T.; Tamaki, T. *Macromolecules* **1996**, *29*, 892.
(18) Böhm, N.; Materny, A.; Kiefer, W.; Steins, H.; Müller, M. M.; Schottner, G. *Macromolecules* **1996**, *29*, 2599.
(19) Mita, I.; Horie, K.; Hirao, K. *Macromolecules* **1989**, *22*, 558.
(20) Ueda, M.; Kim, H. B.; Ikeda, T.; Ichimura, K. *J. Non-Cryst. Solids* **1993**, *163*, 125.
(21) Williams, G.; Watts, D. C. *Trans. Faraday Soc.* **1970**, *66*, 80.
(22) Natansohn, A.; Rochon, P.; Gosselin, J.; Xie, S. *Macromolecules* **1992**, *25*, 2268.
(23) Xie, S.; Natansohn, A.; Rochon, P. *Macromolecules* **1994**, *27*, 1489.
(24) Xie, S.; Natansohn, A.; Rochon, P. *Macromolecules* **1994**, *27*, 1885.
(25) Buffeteau, T.; Desbat, B.; Pézolet, M.; Turlet, J. M. *J. Chim. Phys.* **1993**, *90*, 1467.
(26) Schönhoff, M.; Mertesdorf, M.; Lösche M. *J. Phys. Chem.* **1996**, *100*, 7558.
(27) Lagugné Labarthet, F.; Sourisseau, C. *J. Raman Spectrosc.* **1996**, *27*, 491.
(28) Yam, R.; Cohen, R.; Berkovic, G. *Nonlinear Opt.* **1994**, *00*, 1.
(29) Loucif-Saïbi, R.; Nakatani, K.; Delaire, J. A.; Dumont, M.; Sekkat, Z. *Chem. Mater.* **1993**, *5*, 229.
(30) Fischer, E. *J. Phys. Chem.* **1967**, *71*, 3704.
(31) Ward, I. M. *Structure and properties of oriented polymers*; John Wiley: New York, 1975.
(32) Ward, I. M. In *Advances in Polymer Science*; Kausch, Ed., Springer-Verlag, Berlin, 1985; pp 81−115.
(33) Nagai, H *J. Appl. Polym. Sci.* **1963**, *7*, 1697.
(34) Havriliak, S.; Roman, Jr. and N. *Polymer* **1966**, *7*, 387.
(35) Schneider, B.; Stokr, J.; Schmidt, P.; Mihailov, M.; Dirlikov, S.; Peeva, N. *Polymer* **1979**, *20*, 705.
(36) Dybal, J.; Krimm, S. *Macromolecules* **1990**, *23*, 1301.
(37) Gruger, A.; Le Calvé, N.; Dizabo, P. *J. Chim. Phys.* **1972**, *69*, 291.
(38) Lorriaux, J. L.; Merlin, J. C.; Dupaix, A.; Thomas, E. W. *J. Raman Spectrosc.* **1979**, *8*, 81.
(39) Cataliotti, R. S.; Murgia, S. M.; Paliani, G.; Poletti, A.; Zgierski, M. Z. *J. Raman Spectrosc.* **1985**, *16*, 251.
(40) Socrates, G. *Infrared Characteristic Group Frequencies*, John Wiley: Chichester, England, 1980.
(41) Ho, M. S.; Natansohn, A.; Rochon, P. *Macromolecules* **1995**, *28*, 6124.
(42) Ho, M. S.; Natansohn, A.; Barrett, C.; Rochon, P. *Can. J. Chem.* **1995**, *73*, 1773.
(43) Dhinojwala, A.; Wong, G. K.; Torkelson, J. M. *Macromolecules* **1993**, *26*, 5943.
(44) Dhinojwala, A.; Wong, G. K.; Torkelson, J. M. *J. Chem. Phys.* **1994**, *100*, 6046.
(45) Singer, K. D.; King, L. A. *J. Appl. Phys.* **1991**, *70*, 3251.
(46) Ghebremichael, F.; Kuzyk, M. G. *J. Appl. Phys.* **1995**, *77*, 2896.
(47) Wiesner, U.; Antonietti, M.; Boeffel, C.; Spiess, H. W. *Makromol. Chem.* **1990**, *191*, 2133.
(48) Ho, M. S.; Natansohn, A.; Rochon, P. *Macromolecules* **1996**, *29*, 44.
(49) Barrett, C.; Natansohn, A.; Rochon, P. *Chem. Mater.* **1995**, *7*, 899.
(50) Rochon, P.; Bissonnette, D.; Natansohn, A.; Xie, S. *Appl. Opt.* **1993**, *32*, 7277.
(51) Spevacek, J.; Schneider, B. In *Advances in Colloid and Interface Science*, Elsevier Science Publishers: Amsterdam, 1987; Vol. 27, p 81.

MA980843Z